

and downshifted in the opposite case. Both directions of frequency shift have been observed in our experiments.

Experiment: The heterodyne system of Fig. 2 was used to demonstrate the performance of the optical fibre frequency

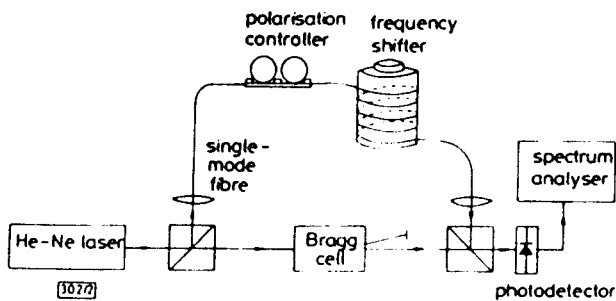


Fig. 2 Heterodyne interferometer for evaluation of frequency shifter

shifter. A fibre polarisation controller and the frequency shifter of Fig. 1 are placed in one arm of a Mach-Zehnder interferometer, with a bulk Bragg cell, centred at 80 MHz, in the second arm.

The frequency shifter has a hollow aluminium cylinder of outer diameter 29 mm and thickness 0.5 mm serving as a former. Jacketed single-mode fibre of 125 μm outer diameter is helically wound on the former. The winding has five turns with a pitch of 2.5 mm. The angle between the acoustic wavefront and fibre is therefore 1.57°. The PZT used is a disc of diameter 10 mm, and is driven at a frequency of 1.6 MHz with a drive power of 0.4 W. The transducer is operated in its thickness mode, launching a travelling acoustic wave into the cylinder. Damping putty is used to eliminate unwanted reflections of the acoustic wave.

Figs. 3a and b show spectrum analyser traces of the

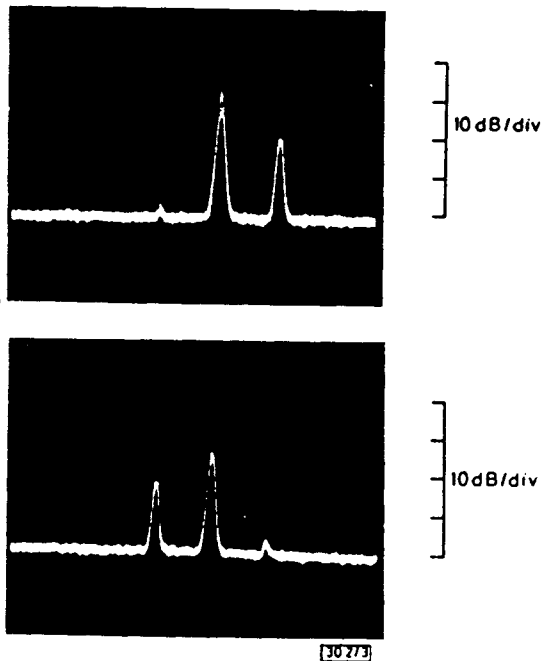


Fig. 3 Spectrum analyser traces showing (a) lower sideband suppressed by 20 dB and (b) upper sideband suppressed by 20 dB

80 MHz carrier with dominant upper and lower sidebands separated from the carrier by 1.6 MHz. In each case the unwanted sideband is suppressed by 20 dB. The required sideband can be selected by adjustment of the polarisation controller, enabling light to be coupled into the induced fast of slow axis of the fibre.

Conversion efficiency, defined as the ratio of optical power in the desired sideband to the input optical power, is estimated to be a few per cent. The low efficiency is due to a number of factors. The polarisation controllers do not provide the adjustment accuracy required to orient the incoming light in the direction of the induced principal axes of the fibre. Also, for optimum operation, the stress generated by the acoustic wave should be at 45° to the fibre axes. This is not the case in

our set-up. Finally, we estimate that there are only two beat lengths in the interaction length of the fibre with the acoustic wave, thereby reducing the conversion efficiency.

In any practical application, an in-line fibre polariser would be placed immediately after the frequency shifter to remove the residual carrier and unwanted sideband which would lie in the orthogonal polarisation to the desired sideband. The novelty of our device lies in the fact that, by using ordinary single-mode fibre, formers of different diameters and windings of different pitch, the phase match conditions of eqns. 4 and 5 can be tailored to suit a large range of acoustic frequencies.

In conclusion, an acousto-optic frequency shifter has been demonstrated using ordinary single-mode fibre with locally induced birefringence. Initial experimental results show 20 dB suppression of the unwanted sideband and conversion efficiency of a few per cent.

J. JI
D. UTTAM
B. CULSHAW

5th September 1986

Department of Electronic & Electrical Engineering
University of Strathclyde
Royal College Building
204 George Street, Glasgow G1 1XW, United Kingdom

References

- 1 CAHILL, R. F., and UDD, E.: 'Solid state phase nulling optical gyro', *Appl. Opt.*, 1980, 19, pp. 3054-3056
- 2 WONG, K. K., DE LA RUE, R. M., and WRIGHT, S.: 'Electro-optic waveguide frequency translator in LiNbO₃ fabricated by proton exchange', *Opt. Lett.*, 1982, 7, pp. 546-548
- 3 NOSU, K., RASHLEIGH, S. C., TAYLOR, H. F., and WELLER, J. F.: 'Acousto-optic frequency shifter for single-mode fibres', *Electron. Lett.*, 1983, 19, pp. 816-818
- 4 RISK, W. P., YOUNGQUIST, R., C., KINO, G. S., and SHAW, H. J.: 'Acousto-optic frequency shifting in birefringent fibre', *Opt. Lett.*, 1984, 9, pp. 309-311
- 5 KIM, B. Y., BLAKE, J. N., ENGAN, H. E., and SHAW, H. J.: 'All-fibre acousto-optic frequency shifter', *ibid.*, 1986, 11, pp. 389-391
- 6 DAKIN, J. P., WADE, C. A., and HAJI-MICHAEL, C.: 'A fibre optic serrodyne frequency translator based on a piezoelectrically strained fibre phase shifter', *IEE Proc. J., Optoelectron.*, 1985, 132, pp. 287-290
- 7 LEFEVRE, H. C.: 'Single-mode fibre fractional wave devices and polarisation controllers', *Electron. Lett.*, 1980, 16, pp. 778-780

CURRENT SENSORS USING HIGHLY BIREFRINGENT BOW-TIE FIBRES

Indexing terms: Optical fibres, Birefringence, Optical sensors, Faraday effect

A fibre with strong elliptical birefringence can be obtained by spinning a linearly birefringent fibre during the draw. Theoretical and experimental results show that such fibres are particularly useful for magnetic field and electric current sensing, since they are resistant to external mechanical perturbations.

Introduction: Optical-fibre current sensors are ideal for use in the electricity generating industry and other hostile environments^{1,2} since they are lightweight, flexible, have large bandwidth and are electrically insulating. Fibre current transducers utilise the Faraday effect, i.e. the rotation of linearly polarised light when the direction of propagation is aligned to a magnetic field. However, the Faraday rotation in a fibre coil is small and is easily quenched by the presence of linear birefringence induced by core ellipticity, asymmetric stress,³ coiling or packaging. Consequently, special fibres designed to overcome these problems are of particular interest.

Spinning a conventional single-mode fibre with moderate linear birefringence has been shown to create a very low birefringence fibre.³ However, the fibre remains as sensitive as

a normal fibre to external effects, e.g. coiling, applied stress and vibration. These effects can be avoided in helical-core fibres⁴ which exhibit sufficiently high circular birefringence to swamp the externally and internally induced linear birefringence. However, the diameter of the fibre has to be large enough to contain the helical core, and therefore it restricts applications to coils of 30 cm radius. Moreover, care has to be taken in launching and splicing.

We report here a further development, the production of spun bow-tie fibres which exhibit a high elliptical birefringence. The fibres are designed to be nearly circularly birefringent, a compromise which ensures good magnetic-field sensitivity while maintaining a high resistance to external perturbations caused by packaging. These attributes allow small-diameter multiturn coils to be used without paying special attention to induced birefringence. Coils having hundreds of turns are easily constructed, thus making fibre current sensors for very low currents a practical reality.

Theory: A strong elliptically birefringent fibre can be fabricated by spinning a fibre having high linear birefringence (e.g. a bow-tie fibre) during drawing. This results in a fibre with a permanent frozen-in rotation of the birefringent axes. The polarisation eigenmodes of such a fibre are elliptically polarised, the elliptical birefringence being dependent on the linear birefringence of the unspun fibre and the rate of twist. Using coupled-mode analysis and the matrix transformation,⁵ the beat length L'_p between the elliptically polarised modes of the spun fibre is given in terms of the beat length L_p of the unspun fibre by

$$L'_p = L_p L_s / \{(4L_p^2 + L_s^2)^{1/2} - 2L_p\} \quad (1)$$

where L_s is the spin pitch.

The beat length L'_p is a measure of the resistance to external perturbations, and should normally be less than 10 mm. The elliptical mode beat length is shown in Fig. 1 as a function of

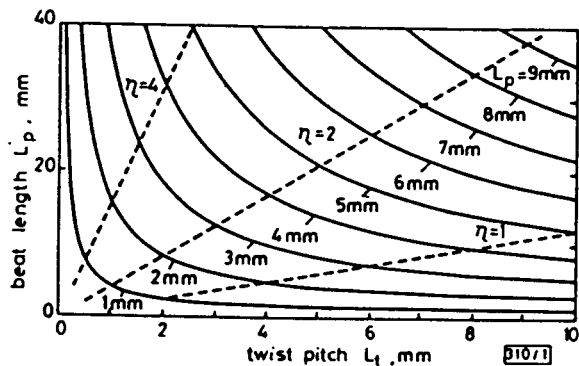


Fig. 1 Calculated resultant elliptically polarised beat length L'_p against spin pitch L_s for various values of unspun fibre beat length L_p .

Values of $2L_p/L_s$ are also shown

the spin pitch L_s for various values of unspun beat length L_p . Curves for values of the ratio $2L_p/L_s$ from 1 to 4 are also shown, and it can be seen that, provided the spin pitch is not less than the unspun beat length, an acceptable increase in fibre beat length of four times results from the spinning process. A bow-tie fibre thus remains highly (elliptically) birefringent. The ellipticity (minor/major axis) of the eigenmodes is given by

$$\epsilon = \tan \left\{ \frac{1}{2} \tan^{-1} (2L_p/L_s) \right\} \quad (2)$$

At high spin rates ($2L_p/L_s > 2$) the ellipticity approaches unity, and the modes are therefore predominantly circularly polarised. Intuitively, little quenching of the Faraday effect might be expected to occur. This can be seen more clearly in Fig. 2, where the calculated relative current sensitivity³ of the fibre in a current monitor is shown for various values of $2L_p/L_s$. The arrangement assumed to detect the Faraday rotation is that described in Reference 1. It can be seen that the sensitivity in the linear region (Faraday rotation angle $< 20^\circ$) differs little from the perfect isotropic fibre ($2L_p/L_s = \infty$) for values of $2L_p/L_s$ greater than about 2. This value corresponds to a

resultant elliptical beat length $L'_p = 4.24L_p$. Thus, to ensure a sufficiently large elliptical birefringence ($L'_p < 10$ mm), one needs to choose a fibre whose unspun beat length L_p is less than about 3 mm.

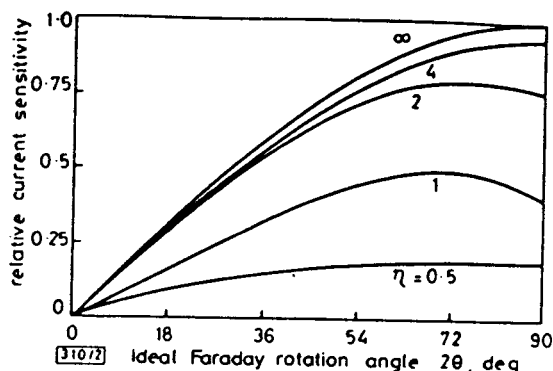


Fig. 2 Relative current sensitivity of a spun highly birefringent fibre for various beat length ratios $2L_p/L_s$.

Curves are for very large total spin number (> 1000)

Experiment: Several different elliptically birefringent fibres have been designed and fabricated by spinning bow-tie fibres. The initial linearly birefringent beat lengths of the fibres ranged from 1.8 mm to 3 mm (at 633 nm) and the spin pitches from 0.9 mm to 7.7 mm. The values of $2L_p/L_s$ were (a) 2.4, (b) 1.1 and (c) 0.46. Fibres were wound into coils with diameters of 3.3 cm and 5.5 cm around a current-carrying conductor. The number of turns on the coils were (a) 100, (b) 140 and (c) 60. The coil leads were about 1 m long. Currents ranging from less than 10 mA to over 400 A were measured by detecting the rotation angle (at 633 nm) of the output state of polarisation.

Fig. 3 shows the experimental results for mains-frequency

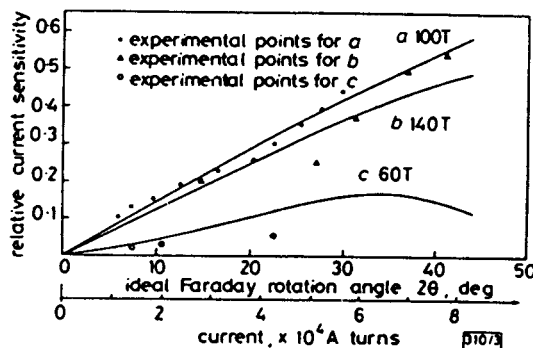


Fig. 3 Experimental results for three spun bow-tie fibres

Solid lines are theoretical calculations

high-current measurements compared with theoretical curves. Here the relative amplitude at the output of the polarisation detector is plotted as a function of the Faraday rotation angle $\theta = 2.65 \times 10^{-4} NI$ for an isotropic fibre, where I is the current and N is the number of turns in the fibre coil. The observed discrepancies are largely due to instability in the HeNe light source and thermal drift (see below).

Currents of less than 10 mA at frequencies up to 2 MHz have also been measured using fibre coil (a) and a 13-turn wire coil having a 20 cm diameter. The system was dominated by laser amplitude noise, which was not compensated by the usual method.¹ Nevertheless, a noise equivalent current of $450 \mu\text{A}/\text{Hz}^{1/2}$ was observed for a current input at a frequency of 30 kHz.

Since the linear birefringence of a bow-tie fibre is temperature-sensitive, some form of temperature compensation will be needed in a practical device to reduce the instability of the output polarisation state. This was achieved by bifilar-winding two identical fibres with opposite spin directions. The fibres were spliced together with their principle axes orthogonal to interchange fast and slow axes. The temperature-compensated fibre coil (coil b) was found to have considerably reduced temperature sensitivity, and normal laboratory temperature fluctuations were no longer a problem.

Conclusion: Spun bow-tie fibres exhibit high elliptical birefringence, which permits measurement of Faraday rotation while retaining resistance to perturbations due to packaging. Coils of up to 140 turns with diameters down to 33 mm have been made and used to measure currents from 10 mA to 400 A. The new fibre has considerable potential for use in sensitive current monitors employing small-diameter multiturn coils, as well as in more conventional current-measuring applications.

Acknowledgment: The authors would like to thank Prof. W. A. Gambling for his valuable suggestions. Thanks are also due to Dr. G. Wylangowski, Mrs. L. Poyntz-Wright and Mr. R. Bailey for fabricating the fibres.

L. LI
J.-R. QIAN*
D. N. PAYNE

8th September 1986

Department of Electronics & Information Engineering
University of Southampton
Highfield, Southampton SO9 5NH, United Kingdom

* On leave from the Department of Radio & Electronics, University of Science & Technology of China, Hefei, Anhui, People's Republic of China

References

- 1 PAPP, A., and HARMS, H.: 'Magneto-optical current transformer', *Appl. Opt.*, 1980, 19, pp. 3729-3745
- 2 ROGERS, A. J.: 'Optical measurement of power-systems quantities', *Electron. & Power*, 1986, 32, pp. 140-144
- 3 PAYNE, D. N., BARLOW, A. J., and RAMSKOV HANSEN, J. J.: 'Development of low and high birefringence optical fibres', *IEEE J. Quantum Electron.*, 1982, QE-18, pp. 477-488
- 4 VARNHAM, M. P., BIRCH, R. D., and PAYNE, D. N.: 'Helical-core circularly-birefringent fibres'. Proc. IOOC-ECOC, Venice, 1985
- 5 HUANG, H. C., and QIAN, J. R.: 'Theory of imperfect nonconventional single-mode optical fibres', in 'Optical waveguide sciences' (Martinus Nijhoff, The Hague, 1983), pp. 57-68

HIGH-SPEED 1.3 μm DFB LASER WITH MODIFIED DCPBH STRUCTURE

Indexing terms: Semiconductor lasers, Optical communications, Optical modulation

High-performance distributed feedback (DFB) double-channel planar buried-heterostructure (DCPBH) lasers ($\lambda = 1.3 \mu\text{m}$) with a modulation bandwidth as high as 5 GHz are reported. The frequency response of these InGaAsP/InP lasers is improved by formation of a double-channel (DC) DCPBH structure with a 20 μm-wide mesa. Threshold currents range between 17 mA and 35 mA. Single-mode operation is observed over a temperature range of 100 K with a sidemode suppression of better than 36 dB at 25°C.

Introduction: Optical fibre transmission of high bit rates over long distances necessitates lasers with single-longitudinal-mode operation. Attractive light sources for this purpose are DFB lasers because of their stable longitudinal mode operation. Low threshold currents and high-power operation have been reported for InGaAsP/InP DFB lasers.^{1,2} However, high-speed modulation presents a severe problem for all types of buried-heterostructure (BH) lasers because of the large parasitic capacitance of the blocking layers. Earlier attempts to improve the high-frequency behaviour of DCPBH lasers by formation of a double-channel (DC) DCPBH structure resulted in a 3 dB rolloff below 3 GHz,³ whereas ion bombardment³ and mesa etching⁴ led to an improved 3 dB rolloff at about 3 GHz. In this letter a DFB-DC-DCPBH laser is reported with improved high-frequency modulation characteristics and stable DFB operation over a large temperature range.

Device technology: A schematic diagram of the realised high-frequency DFB laser structure with a DC-DCPBH configuration is shown in Fig. 1. A second-order grating (period

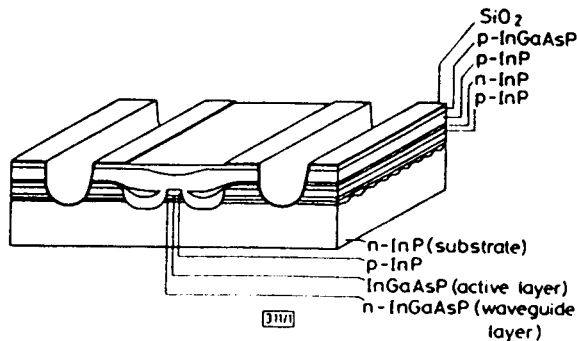


Fig. 1 Schematic cross-section of a DFB-DC-DCPBH laser

around 400 nm) is formed along the (011) direction on a (100)-oriented *n*-doped substrate by holographic lithography and wet chemical etching. In a first liquid-phase-epitaxial (LPE) step, the corrugated substrate is overgrown with an *n*-InGaAsP waveguide layer ($d_w = 0.12 \mu\text{m}$, $\lambda = 1.15 \mu\text{m}$), followed by the undoped active InGaAsP layer ($d_a = 0.12 \mu\text{m}$, $\lambda = 1.3 \mu\text{m}$) and a *p*-InP layer ($d = 0.5 \mu\text{m}$). The 900 Å corrugation depth of the sinusoidal grating is conserved during LPE overgrowth by applying a GaAs cover. After etching the inner double channels which define a 2 μm-wide mesa in the (011) direction, the InP current blocking layers and the *p*-InGaAsP cap layer are grown in a second LPE step,⁵ resulting in a conventional DCPBH structure.

Parasitic capacitances associated with the *pn* junctions in the current blocking layers are efficiently reduced by etching two 8 μm-deep channels which define a 20 μm-wide mesa (Fig. 1). Thus, the blocking layers outside this mesa are electrically separated from the active region, and afterwards isolated by a 400 nm-thick SiO₂ layer. Above the laser stripe a 14 μm-wide contact window is opened in the SiO₂. After Zn-diffusion into the InGaAsP cap layer, *p*- and *n*-contact metallisation is performed with identical contact metals consisting of Ti/Au. Since no alloying is necessary after evaporation, deterioration of the layer properties (as sometimes observed after alloying) is prevented.

The length and width of the cleaved laser chips are 350 μm and 300 μm, respectively. The chips are mounted upside-down on Au-plated Cu submounts. Antireflection (AR) coating on both facets of the mounted laser chips is performed by a low-temperature (80°C) plasma-enhanced deposition of SiN_x ($n = 1.85$).

Results: The light/current characteristic of a DFB-DC-DCPBH laser is shown in Fig. 2, together with the mode spectra (log scale) at 4 mW and 10 mW output powers. A threshold

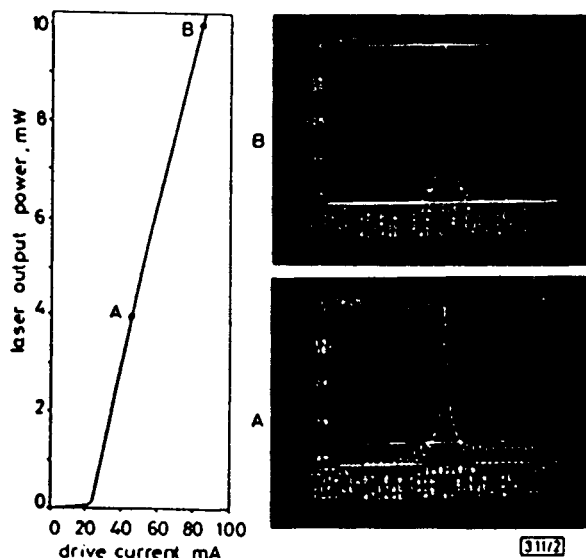


Fig. 2 Laser output against current characteristics (25°C, CW) and mode spectra at 4 mW and 10 mW output powers